Macromolecular Bioscience 2021; 21:2000379 (4): pp. 1-10 (DOI: 10.1002/mabi.202000379)

The effect of electron beam (E-beam) irradiation-induced sterilization on the morphological, chemical, mechanical, optical and biological properties of PMMA

Sina Sharifi[1], Mohammad Mirazul Islam[1], Hannah Sharifi[1], Rakibul Islam[2], Tahmida N. Huq[3], Per H. Nilsson[2,4], Tom Eirik Mollnes[2,5,6], Khoa D. Tran[7], Corrina Patzer[7], Claes H. Dohlman[1], Hirak K. Patra[8], Eleftherios I. Paschalis[1], Miguel Gonzalez-Andrades[1, 9], and James Chodosh[1*]

[1]Disruptive Technology Laboratory, Massachusetts Eye and Ear and Schepens Eye Research Institute, Department of Ophthalmology, Harvard Medical School, Boston, MA, USA
[2]Department of Immunology, Oslo University Hospital, Rikshospitalet, University of Oslo, Oslo, Norway
[3]Department of Materials Science and Metallurgy, University of Cambridge, Cambridge, UK
[4]Linnaeus Center for Biomaterials Chemistry, Linnaeus University, Kalmar, Sweden
[5]Research Laboratory, Nordland Hospital, Bodø, and Faculty of Health Sciences, K.G. Jebsen TREC, University of Tromsø, Norway.
[6]Centre of Molecular Inflammation Research, Norwegian University of Science and Technology, Trondheim, Norway.
[7]Vision Research Laboratory, Lions VisionGift, Portland, OR, USA
[8]Department of Chemical Engineering and Biotechnology, Cambridge University, Cambridge, UK
[9]Maimonides Biomedical Research Institute of Cordoba (IMIBIC), Department of Ophthalmology, Reina Sofia University Hospital and University of Cordoba, Cordoba, Spain

*Corresponding author. James Chodosh, MD MPH, Massachusetts Eye and Ear, Boston, MA, 02114, USA.
E-mail: James_Chodosh@meei.harvard.edu

Abstract

Electron beam (E-beam) irradiation is an attractive and efficient method for sterilizing implantable medical devices made of natural or synthetic materials, such as poly (methyl methacrylate) (PMMA). As the ionizing irradiation can affect the chemical structure of PMMA, understanding the consequences of E-beam sterilization on the intrinsic properties of PMMA is vital for clinical implementation. In this study, we report a detailed assessment of the chemical, optical, mechanical, morphological, and biological properties of medical-grade PMMA after E-beam sterilization at 25 and 50 kiloGray (kGy). Fourier transform infrared spectroscopy, thermogravimetric analysis, and differential scanning calorimetry studies indicate that E-beam irradiation has minimal effect on the chemical properties of the PMMA at these doses, while at 25 kGy the mechanical and optical properties of the PMMA remain unaltered. However, at 50 kGy the flexural strength and transparency were reduced by 10 and 2%, respectively. Atomic force microscopy demonstrates that E-beam irradiation reduces the surface roughness of PMMA in a dose dependent manner. Live-Dead, AlamarBlue, immunocytochemistry, and complement factor activation studies show that E-bean irradiation up to 50 kGy has no adverse effect on the biocompatibility of the PMMA. These findings suggest that E-beam irradiation at 25 kGy may be a safe and efficient alternative for PMMA sterilization.

Introduction

The irradiation of organic polymers intended for medical use, with ionizing irradiation such as E-beam often cause the formation of reactive intermediates including free radicals, ions, and atoms in excited states.[1] These intermediates can undergo various chemical reactions such as disproportionation, hydrogen abstraction, rearrangements, and breaking and/or formation of new chemical bonds. This is beneficial when it alters the macromolecular structures present in contaminating pathogens, as it eradicates any bio-burden, and sterilizes medical packaging.[2] However, such chemical reactions can also modify polymer structures and their properties, depending on the structure of the polymer, exposure dose, duration time, and the irradiation conditions.[1, 3] One of the most widely used polymers in medical technologies and implants is poly (methyl methacrylate) (PMMA). This is due to its excellent biocompatibility, reliability, relative ease of manipulation, and low toxicity.[4] Some of the most common application of PMMA in medical technologies are in: (*i*) keratoprosthesis,[5] (*ii*) contact and

intraocular lens,[6] (*iii*) orthopedic,[7] (*iv*) dental, [4] and (*v*) plastic surgery.[8] PMMA-made implants typically come into direct contact with the blood stream or are contained in avascular body compartments, and therefore must be sterilized prior to their application.

There are numerous sterilization methods including steam, dry heat, pressured vapor, ethylene oxide (EtO), H_2O_2 gas plasma, peracetic acid exposure, as well as irradiation – either gamma or E-beam. Effective sterilization must eliminate all infectious agents, including bacteria, viruses, fungi, and parasites, without damaging the intrinsic properties of the material.[9] EtO is preferred for sensitive materials that cannot tolerate heat, and thus it is a commonly applied method for sterilization of PMMA-made medical devices,[10] for example the Boston keratoprosthesis, a device used to replace a diseased cornea when corneal allograft surgery fails.[11] However, EtO sterilization is a slow and expensive process and requires careful handling of EtO due to its toxicity and flammability. Thus, ventilation and aeration are necessary to purge the gas which adds to the cost.[9] In contrast, gamma irradiation has been shown to be a feasible and tractable method to sterilize PMMA devices.[10b, 12] However, concerns remain around induced yellowing when the device is for optical purposes.

E-beam irradiation is an attractive, emission free, and faster sterilization alternative for medical devices, compatible with low temperature requirements for plastics.[13] E-beam irradiation allows full control of the dose and temperature during sterilization.[9] It has been shown that PMMA can reasonably tolerate a single irradiation sterilization dose, although not for repeated sterilizations.[14] It was also shown that the E-beam irradiation can affect mechanical and optical properties of industrial PMMA.[15] However, whether the level of E-beam irradiation sufficient to achieve sterilization to regulatory standards, has any clinically relevant effect on the properties of medical-grade PMMA has not been fully studied. Thus, considering the recommended dose for terminal sterilization of medical products is 25 kGy dose that guarantees a Sterility Assurance Level (SAL) of 10^{-6},[9] we herein irradiated the PMMA for 25 and 50 kGy and studied the effect on its chemical, mechanical morphological, optical, and biological properties.

Methods

E-beam Irradiation. Medical grade PMMA (Rod number 2, PolyOne; Littleton, MA) discs with 0.5 mm thickness and 40.0 mm diameter were acquired from JG Machine Company (Wilmington, MA). The PMMA disks were placed and sealed in Medical Pouches (Steriking SS-T 4A; Helsinki, Finland), placed on an aluminum carrier tray, and irradiated using a Van de Graaff (Model K) electron accelerator (Electron Technology Company; South Windsor, CT) at 2.6 Mev with the dose rate of 5 kGy per pass (5, and 10 passes to reach 25 and 50 kGy irradiation, respectively).

Fourier Transform Infrared Spectroscopy (FT-IR). FT-IR spectra of the PMMA discs (non-irradiated, 25 and 50 KGy irradiated) were collected in the range from 500 to 4000 cm^{-1} using a Nicolet iS50 FT-IR Spectrometer (Thermo Scientific; Waltham, MA) equipped with all-reflective diamond Attenuated Total Reflectance (ATR). Spectra were acquired *via* OMNIC software (Thermo Scientific) with 64 scans and 0.5 cm^{-1} resolution after spectral correction with ambient atmosphere.

Water Contact Angle Measurement: The contact angle measurements were carried out by a Contact Angle and Surface Tension Measurement System (FTA100, First Ten Angstroms, Portsmouth, VA) using a static sessile drop technique. At room temperature, 5 μL size droplet of distilled water was dropped by a syringe, located above the sample surface, and then a high-resolution camera used to capture an image from the side. The contact angle was analyzed and recorded using FTA 2.1 software and averaged for each group [n = 4].

Optical Transmission. The transmission of the PMMA discs (0, 25 and 50 KGy irradiated) was assessed by a UV-Vis spectrometer (Molecular Devices SpectraMax 384 Plus Microplate Reader; Molecular Devices, San Jose, CA). First, PMMA discs were cut to 6.0 mm diameter by a laser cutter (Helix 75W Laser Cutter; Epilog, Golden, CO), then placed in a 96-well quartz microplate, and their optical transmittance was recorded from 250-850 nm in a quartz microplate at 1-nm wavelength increments at varying time points (1-60 days) after irradiation. The transmittance of the samples [n = 4] was corrected with blank media (air) and the mean transmittance (%) for each group was calculated and plotted as a function of wavelength.

Atomic Force Microscopy (AFM). The morphology of the PMMA discs (0, 25 and 50 KGy irradiated) was probed by an AFM instrument (Asylum Research Cypher - Oxford Instruments, High Wycombe, UK) in the AC mode. The data was acquired in phase and height profiles with scan size of 10×10 μm^2 and rate of 2.0 Hz.

Thermal Gravimetric Analysis (TGA). TGA was performed using a TA Instruments TGA Q50 (New Castle, DE). Samples weighing between 2.3-3.5 mg, were initially heated in a platinum pan at a rate of 10 °C/min to reach 100 °C, and kept isothermal for 15 mins in argon with a flow rate of 80 mL/min. The temperature was then increased to 600 °C at a rate of 20 °C/min under argon.

Differential Scanning Calorimetry (DSC). DSC measurements were performed using a TA Instruments DSC Q20 thermal analyser (New Castle, DE). The PMMA samples were cut into 4.0 mm diameter disks, weighed using a Sartorious balance (Göttingen, Germany), and encapsulated in crimped aluminium pans. An empty pan was used as a reference. The temperature system was allowed to equilibrate at 0° C and remained isothermal to 10 mins before being ramped to 250° C at 10 °C/min under an argon flow of 80 ml/min.

Mechanical Properties. The mechanical properties of PMMA before and after varying E-beam irradiation were assessed using standard three-point bending flexure test.[16] First, PMMA discs (0, 25 and 50 KGy irradiated) were cut to rectangle shapes (15×4 mm) with the thickness of 0.5 mm using a Helix 75W laser cutter, placed on the two-point holder, and fixed on the stationary stage of a mechanical tester (Mark-10 ESM 303; Copiague, NY). A longitudinal downward force was applied using the flathead loading pin from the mobile stage with crosshead speed of 2 mm/min. The applied force as function of displacement was recorded and used to calculate the flexural modulus and strength of the specimens [n = 8].

In-vitro Biocompatibility

Live-Dead Assay. To assess the biocompatibility of the PMMA before and after E-beam irradiation with respect to human corneal fibroblasts (HCF) and human corneal epithelial cells (HCEp), we performed a standard Live-Dead assay. After E-beam irradiation of 8.0 mm PMMA discs, they were placed in 48-cell culture well plates and washed with sterile phosphate buffered saline (PBS) solution. Next, 10,000 HCF or HCEp were seeded on each disc in 20 μL of appropriate media (*i.e.* HCF: DMEM media (ATCC; Manassas, VA) supplemented with 10% fetal bovine serum (Gibco; Gaithersburg, MD) and HCEp: serum-free medium (KSFM) supplemented with 50 μg/ml bovine pituitary extract and 5 ng/ml epidermal growth factor (Gibco) and allowed to adhere for 30 min prior to addition of 500 μL of extra media,[10b, 17] followed by incubation at 37 °C and 5% CO_2 for up to 7 days. The cell culture media was changed every other day. Following 1, 4, and 7 days of cell culture, Live-Dead staining was performed (Life Technologies Carlsbad, CA) and imaged using an inverted fluorescent microscope (Zeiss

Axio Observer Z1; Thornwood, NY). Four samples per group (25 and 50 kGy) were examined and compared to those of tissue culture well plate (TCP) and non-irradiated PMMA discs as controls. Cellular viability was assessed using ImageJ software from images obtained from each sample (n = 4), as described previously.[18]

AlamarBlue Assay. To evaluate the metabolic activity of the HCF and HCEp seeded on the PMMA discs (0, 25 and 50 kGy irradiated), we performed a standard AlamarBlue assay. After culturing the cells on the discs, as explained above, the AlamarBlue study was carried out at day 1, 4 and 7 days post-seeding. At each time point, 50 μL of 0.01% w/v resazurin sodium salt (Sigma-Aldrich, St. Louis, MO) was added to the culture plate and incubated for 2 h at 37 °C. Next, 300 μL of that media was transferred to a new 96 well plate (100 μL in each well) and read on a BioTek plate reader (Synergy 2, BioTek Instruments) at 530/25 nm for excitation and 600/25 nm for emission, and corrected for the fluorescence of discs incubated without cells. Twelve samples per group (25 and 50 kGy) were tested and compared to those of TCP and non-irradiated PMMA discs as controls.

Immunocytochemistry (ICC). Specific markers (ALDH3A1, integrin β1, FAK and α -SMA) expressed by HCF seeded on PMMA substrates (non-irradiated, 25 and 50 KGy) were assessed by fluorescence ICC. After culturing cells on the PMMA discs for 6 days as above, the discs were removed from the media, gently washed with PBS, and fixed in 4% paraformaldehyde. Afterwards, they were permeabilized with 0.25% Triton X-100, and treated with 5% Fetal bovine serum in PBS with 0.05% Tween-20 (PBST), followed by incubation with primary antibodies overnight at 4 °C in humidifying conditions. The specific antibodies included: (*i*) mouse monoclonal antibody against ALDH3A1 (clone 1B6; GTX84889, dilution 1:100, GenTex); (*ii*) rabbit polyclonal antibody against Integrin β1 (GTX112971, dilution 1:250, GenTex); (*iii*) rabbit monoclonal antibody against FAK (clone EP695Y; ab40794, dilution 1:250, Abcam); and (*iv*) mouse monoclonal antibody against α-SMA (clone 1A4; ab7817, dilution 1:200, Abcam). Subsequently, the specimens were incubated with FITC-conjugated anti-mouse antibody (ab6785, dilution 1:1000, Abcam), or FITC-conjugated anti-rabbit antibody (ab6717, dilution 1:1000, Abcam) for 1h at room temperature, mounted in VectaShield mounting media containing DAPI (Vector Laboratories) and imaged by an inverted fluorescent microscope (Zeiss Axio Observer Z1).

Ex-Vivo Complement Activation Experiments. Activation of complement by PMMA before and after irradiation was assessed as previously described, using blood from human donors.[19] The ethical committee at Oslo

University Hospital approved the study (REK SØR S-04114), and the research conformed to the Declaration of Helsinki. Informed written consent was obtained from each donor. Human blood was drawn from healthy volunteers into Vacutainer™ tubes (Becton, Dickinson and Co., Plymouth, UK) containing a specific thrombin inhibitor, lepirudin (Refludan®, Aventis Pharma, Mumbai, India) at a final concentration of 50 μg/mL. For each set of experiments, 300 μL of the blood was aliquoted into five cryogenic vials (Thermofisher, MA). In one vial, EDTA was added immediately at 10 mM final concentration to measure the complement activation status at time zero (T0). The other four vials containing whole blood were incubated at 37 °C as follows: non-irradiated and 25, and 50 kGy irradiated PMMA discs were each placed in a vial. The fourth vial was left with only whole blood. After incubation, EDTA was added to stop further complement activation, and plasma was separated for preservation. The incubated whole blood without an immersed specimen served as a negative control for complement activation. A total of five independent experiments were performed at 30 minutes incubation. Collected plasma was preserved at -70 °C. Complement activation was assessed by measuring soluble C3bc fragments, and the soluble terminal complement complex sC5b-9 (TCC), both using ELISA as described previously.[20] C3bc was determined using monoclonal antibody bH6 for capture and polyclonal rabbit anti-C3c (Behringwerke AG, Marburg, Germany) and peroxidase-labeled anti-rabbit immunoglobulin (GE Healthcare, Chicago, IL) as detection antibodies. Levels of sC5b-9 were determined with anti-neo C9 monoclonal antibody aE11 for capture,[21] and biotinylated monoclonal anti-C6 (clone 9C4) as previously described.[20-21] Streptavidin-HRP conjugate (GE Healthcare, Chicago, IL) was added for detection.

Statistical Analysis. One-way ANOVA with Tukey comparison test was used to compare flexural strain and modulus surface roughness, contact angle, viability, metabolic activity, and TCC between groups. A value of $p \leq 0.05$ was considered statistically significant. n.s., *, **, ***, and **** represent $p > 0.05$, $p \leq 0.05$, $p \leq 0.01$, $p \leq 0.001$ and $p \leq 0.0001$, respectively. GraphPad Prism Software (GraphPad Software version 8.3.0, CA, USA) was used to analyze the data.

Results and Discussion

Chemical characterization. The FT-IR spectra of the PMMA specimens are shown in Figure 1a. FT-IR absorbance spectra of non-irradiated and 25 kGy irradiated PMMA samples are almost superimposable. Yet, upon a closer inspection, it is apparent that the C=C stretching vibration at around 1637 cm^{-1} grows after irradiation. This coincides with reduction in the intensity of C–O, C=O bonds groups at 1149 and 1731 cm-1, respectively. Such intensities changes are more predominant with 50 kGy, and suggest that as the E-beam dose increases, the rate of chain scission increases to generate free radicals that recombine to form C=C bonds.[22] Moreover, a broad low-intensity peak appears in the higher energy side of the spectra (3000-4000 cm^{-1}) for PMMA samples after 50 kGy irradiation, suggesting the presence of an OH stretching bond. This may have originated from the oxidative degradation of PMMA during high energy electron bombardment in the presence of atmospheric oxygen.[23] These data suggest that the higher doses of irradiation have an effect on the chemical structure of PMMA.

TGA and TGA derivative plots of non-irradiated and irradiated (25 and 50 kGy) PMMA are co-plotted in Figure 1b. As shown in Figure 1 and Table 1, the irradiation of PMMA with 25 and 50 kGy reduces the onset temperature (T_{10}: temperature at 10% mass loss) from 273.4 to 236.4 and 238.4 °C, respectively. This coincides with the first decomposition stage of the PMMA as indicated by the appearance of the TGA derivative peak at 228.8 and 224.2 °C. This finding is believed to originate from the presence of lower molecular weight and unstable fragments in irradiated PMMA that undergo degradation and evaporation at lower temperatures, as compared to non-irradiated PMMA, in which there was no such change.[23b, 23c, 24] Lower doses of irradiation (25 kGy) appeared to decrease the onset temperature more than those of higher doses (50 kGy). On the other hand, the midpoint temperature (T_{50}: temperature at 50% mass loss) drops for 25 kGy, but increases for 50 kGy. This suggests that at a lower dose of irradiation, chain scission dominates the degradation processes, while at a higher dose, crosslinking of the generated reactive species may occur. Such chain scission and crosslinking are also responsible for reducing and increasing T_{max} (maximum weight loss temperature) in 25 kGy and 50 kGy irradiated PMMA, respectively. Although the thermal behavior of PMMA after E-beam irradiation with varying doses has not been previously studied, prior studies of gamma irradiated PMMA showed similar behavior.[23a, 25]

Table 1: Data Obtained from TGA and DSC Thermograms

Samples	TGA				DCS
	T_{10} (°C)	T_{50} (°C)	T_{max}/°C (°C)		T_g (°C)
			Stage 1	Stage 2	
PMMA	273.4	340.0	-	349.1	131.1
25 kGy	236.4	337.8	228.8	347.9	128.2
50 kGy	238.4	342.8	224.2	353.6	128.3

The DSC thermograms of non-irradiated, 25 and 50 kGy irradiated PMMA along with their corresponding glass transition temperature (T_g), are shown in the Figure 1c. E-beam irradiation of PMMA shifted the T_g from 131.1 °C to 128.2 and 128.3 °C for 25 and 50 kGy, respectively, and altered the slop of heat flow in the DSC curves. The former suggests increase in the mobility of the polymer chains, and the latter indicates the presence of smaller molecular weight species which then can undergo degradation or evaporation.[26] This is in agreement with the TGA studies, validating the dominance of chain scission and crosslinking for 25 and 50 kGy, respectively. Although data suggest that E-beam irradiation affects the thermal properties of the PMMA, this is biologically insignificant, considering that PMMA implants are at body temperature (37 °C).

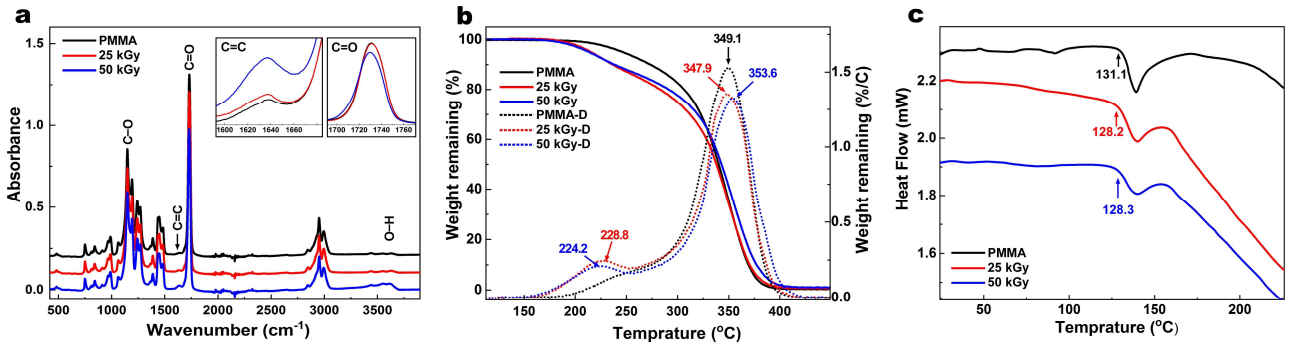

Figure 1. Chemical characterization of PMMA after E-beam irradiation. (**a**) Fourier transform infrared (FT-IR), (**b**) Thermal Gravimetric analysis (TGA), and (**c**) Differential scanning calorimetry (DSC) plots of PMMA before and after 25 or 50 kGy irradiation. Increasing C=C and O-H and reducing C=O and C-O peaks intensities suggest that 50 kGy has a more prominent effect on the chemical structure of the PMMA. Irradiated samples have two decomposition stages compared to one in non-irradiated PMMA, with varying T_{10}, T_{50}, T_{max}, (TGA) and T_g (DSC), suggesting the chain scission and crosslinking in the 25 and 50 kGy, respectively.

Mechanical characterization. To determine whether the E-beam irradiation impacts the mechanical properties of the PMMA, we performed 3-point bending test (Figure 2a) and calculated flexural modulus and strength according to a previously described approach.[16] Figure 1b-d represents the flexural strains for non-irradiated, 25, and 50 kGy irradiated PMMA discs as function of stress. Our data shows that the flexural modulus of non-irradiated, 25, and 50 kGy irradiated PMMA is 5.46 ± 0.48, 5.22 ± 0.35 and 5.10 ± 0.37 GPa, respectively (Figure 1e). Although the apparent gradual decrease in the flexural modulus of PMMA is consistent with a prior study,[15] statistical analysis showed no significant difference between the irradiated and non-irradiated PMMA ($p > 0.05$ for both comparisons). Moreover, 25 and 50 kGy irradiated PMMA samples demonstrate a flexural strength of 0.456 ± 0.024 and 0.427 ± 0.025 GPa, respectively, as compared to 0.470 ± 0.033 GPa of non-irradiated PMMA (Figure 1f). These data suggest that only the 50 kGy was statistically different from non-irradiated PMMA ($p = 0.012$). Thus, irradiation at 25 kGy with E-beam did not significantly change the mechanical properties of PMMA.

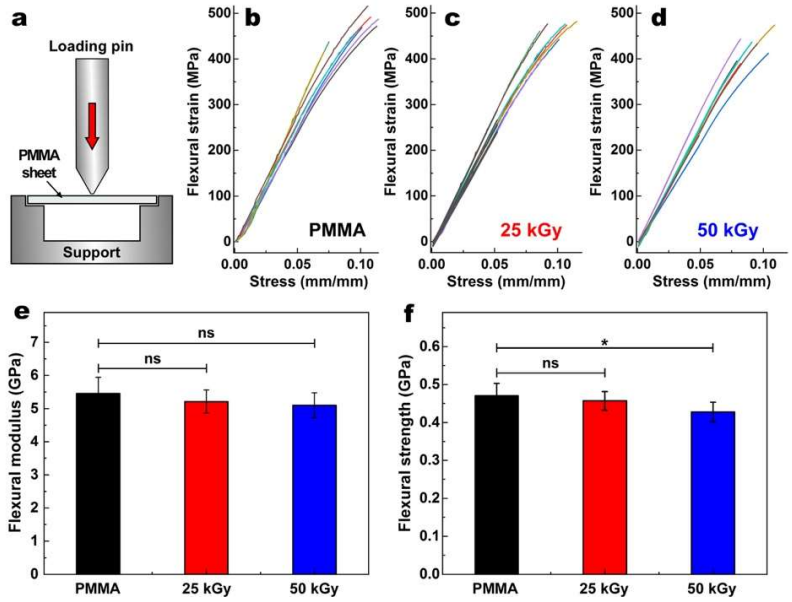

Figure 2. Schematic illustration of standard three-point bending flexure test (**a**). Obtained flexural strain as function of stress for non-irradiated (b), 25 kGy (**c**) and 50 kGy (**d**) irradiated PMMA, and their corresponding flexural moduli (**e**) and flexural strengths (**f**). There was no significant difference in flexural modulus between non-irradiated and 25 and 50 kGy PMMA. ns, and * represent $p > 0.05$, $p \leq 0.05$, respectively.

Optical properties. Optical transmission studies of PMMA discs before and after E-beam irradiation using ultra-violet (UV-Vis) spectroscopy shows that the E-beam irradiation reduces the optical transmission of the PMMA in a dose-dependent manner, as illustrated in Figure 3. The reductions of transmission in the visible range (390-490 nm) was 2.7 ± 0.2 and 6.2 ± 0.3 % for 25 and 50 kGy irradiated PMMA, respectively. However, those reductions were more pronounced 52.7 ± 0.8 and 67.6 ± 1.1 in the ultraviolet (UV) region of spectra (250-350 nm) for both 25 and 50 kGy, respectively. Light transmission reduction in the visible range (390-490 nm) results in yellowing of the PMMA samples after irradiation. However, the yellowing gradually fades away at room temperature within the first 30 days after irradiation (Figure 2), and then the color remains stable for both 25 and 50 kGy samples. While light transmission in the visible range recovered fully in the 25 kGy group, in the 50 kGy group it did not (Figure 3d). The recovery rate in the UV range was dose-dependent, and neither of the two groups (25 and 50 kGy) achieved full recovery. The reduction in transmission originates from the changes in the chemical structure of the PMMA, as indicated by FT-IR, DSC, and TGA studies. This suggests that 25 kGy irradiation does not affect the transmission of visible light, but permanently reduces the transmission of harmful UV light, which would be beneficial for patients. In contrast, the 50 kGy dose permanently reduces the visible and UV transmission. A similar dose of gamma irradiation (25 kGy), on the other hand, was shown to have a significantly greater impact on the optical properties of PMMA, and reduced transmission in the visible range of 350-500 nm by 15.0 ± 0.5 % with only 3.0 ± 0.1 % recovery in 90 days.[10b]

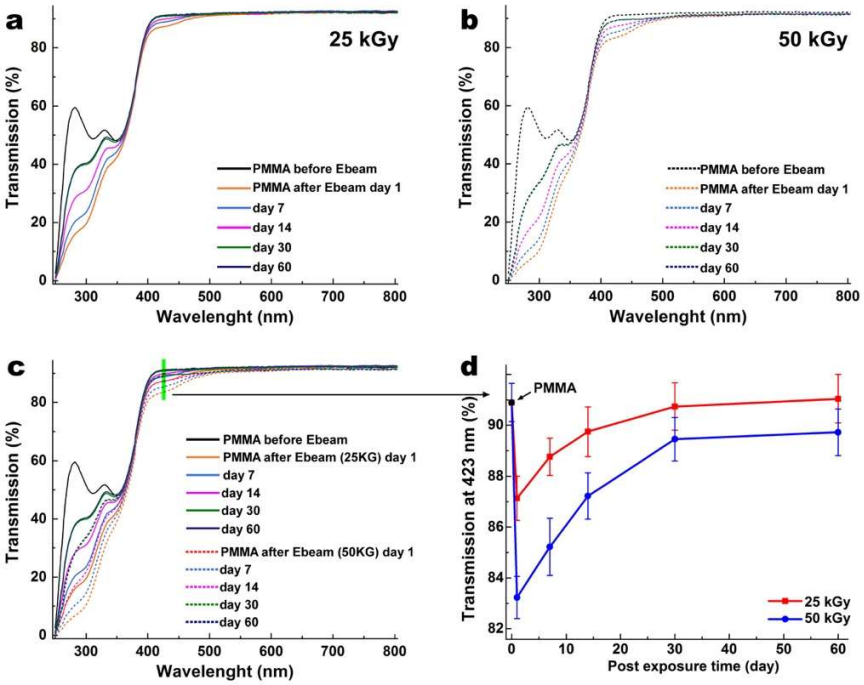

Figure 3. Graphs of optical transmission of PMMA before and after irradiation at 25 kGy (**a**), 50 kGy (**b**), and with both superimposed (**c**) as a function of time to 60 days post treatment, in the range on 250-800 nm. **d**) The recovery of transmission plotted at 423 nm (extracted from (**c**) plot, as shown by green line) after 25 and 50 kGy irradiation. 25 kGy irradiated PMMA samples reach near full recovery after 1 month. The 50 kGy irradiated PMMA recovered 95% of transmission in the blue light area.

Surface properties: Bombardment of the PMMA surface with high energy E-beam irradiation has shown to alter the crosslinking density and chemical and morphologic characteristics of PMMA films, potentially leading to amorphization.[22, 27] To investigate whether E-beam irradiation impacts the morphological properties of medical-grade PMMA, we employed AFM. Our data demonstrate a dose dependent smoothening of the surface after irradiation (Figure 4a-c). The surface roughness analysis showed Root Mean Square (RMS) values of 9.34 ± 2.39, 7.15 ± 1.42, and 5.92 ± 1.79 for non-irradiated, 25 kGy, and 50 kGy irradiated PMMA, respectively, demonstrating that irradiation reduced surface roughness. Contact angle measurements to determine whether E-beam irradiation affected the wettability of the PMMA surface showed slight reductions in the water contact angle from 74.5° ± 3.2° for non-irradiated PMMA to 66.7° ± 2.5°, and 62.6° ± 3.1° for 25 and 50 kGy irradiated samples, respectively. These changes could originate from the change in the chemical and morphological properties of the polymer due to electron bombardment.[28]

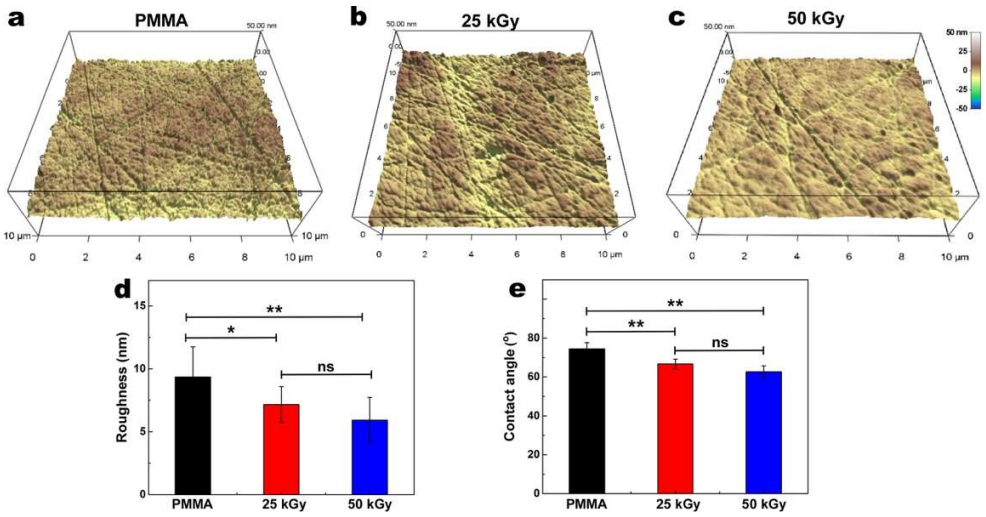

Figure 4. Morphological characterization of PMMA surface before (**a**), after 25 kGy (**b**), and 50 kGy (**c**) irradiation with a scan size of 10×10 μm^2 and their analyzed surface roughness (**d**), using Atomic Force Microscopy (AFM). (**e**) contact angle values of PMMA surfaces before, and after 25 kGy and 50 kGy irradiation. AFM and contact angle studies suggested that irradiation decreases the roughness and contact angle in a dose dependent manner. ns, *, and ** represent $p > 0.05$, $p \leq 0.05$, and $p \leq 0.01$, respectively.

Biocompatibility. Since E-beam irradiation alters the structure and surface properties of PMMA, we assessed the effect of these changes on cytotoxicity and biocompatibility of the PMMA. After culturing human corneal fibroblasts (HCF) on non-irradiated or irradiated PMMA discs (25, and 50 kGy), we performed a Live-Dead assay, and studied the cell viability (Figure 5a-b). Live-Dead analysis (Figure 5b) showed no significant differences between cell viability of non-irradiated, 25, and 50 kGy PMMA discs during 7 days of cell culture (> 90 %), observing similar cell morphology between groups. We also studied the interaction of human corneal epithelial cells (HCEp) with PMMA with and without E-beam irradiation (Figure 5c-d). HCEp seeded on non-irradiated, 25, and 50 kGy irradiated PMMA samples demonstrated similar morphology and viability (> 85%) over 7 days of culture (Figure 5d). These data suggest that E-beam irradiation of PMMA does not lead to increased cytotoxicity or reduce its biocompatibility.

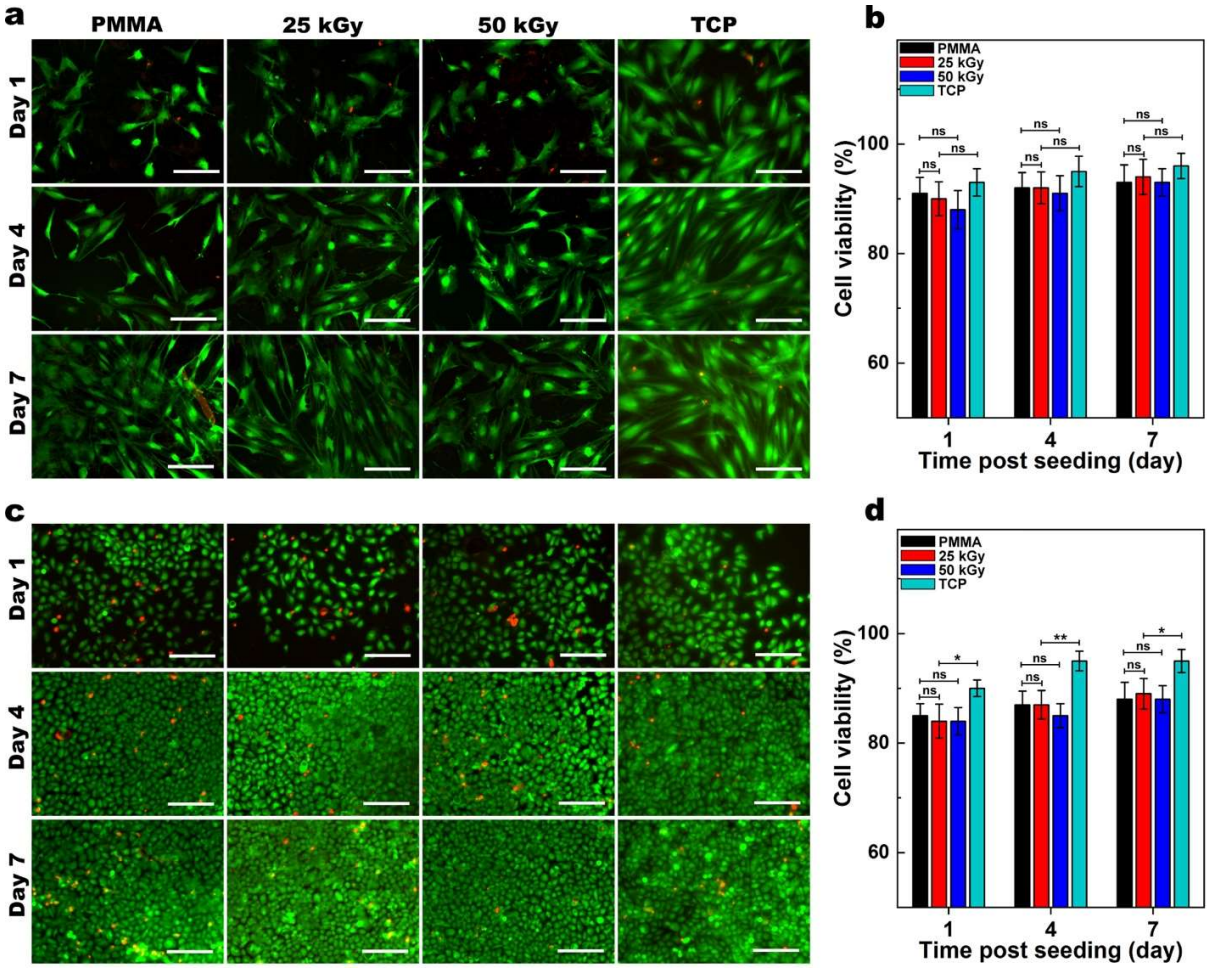

Figure 5. Biocompatibility of PMMA with and without E-beam irradiation. Representative Live/Dead images of human corneal fibroblasts (HCF) (**a**) and human corneal epithelial (HCEp) cells (**c**) cultured on PMMA, with and without 25 or 50 kGy irradiation compared to those cultured on tissue culture plates (TCP), and their corresponding cell viability (**b** and **d**) after 1, 4, and 7 days of cell culture (scale bar: 200 μm). Cells viability was quantified from Live/Dead images using ImageJ (Green [calcein AM]: lived cells; Red [ethidium homodimer-1]: dead cells). ns, *, **, ***, and **** represent $p > 0.05$, $p \leq 0.05$, $p \leq 0.01$, $p \leq 0.001$ and $p \leq 0.0001$.

We further studied the metabolic activity of HCF and HCEp seeded on PMMA with or without irradiation using the AlamarBlue assay. A steady increase in the relative metabolic activity as function of incubation time suggests cellular growth and proliferation over time on all samples. At days 1, 3, and 7, of cell culture, HCF and HCEp grown on 25 and 50 kGy PMMA discs had similar activity to those on non-irradiated PMMA (Figure 6). These results are consistent with the Live-Dead assays, and indicate that 25 and 50 kGy E-beam irradiation do not adversely affect PMMA biocompatibility.

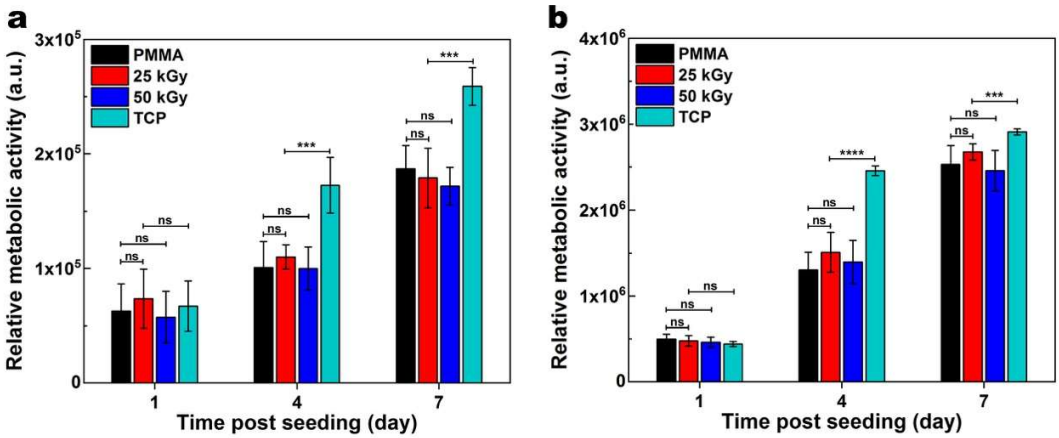

Figure 6. Quantification of the metabolic activity of HCF (**a**), and HCEp (**b**) cultured on PMMA, with or without 25 and 50 kGy irradiation compared to those cultured on tissue culture plate (TCP), using AlamarBlue assay performed at 1, 4, and 7 days of cell culture. The cells seeded on all three surfaces demonstrated similar metabolic activity, suggesting that the irradiation did not diminish biocompatibility of the PMMA. ns, *, **, ***, and **** represent $p > 0.05$, $p \leq 0.05$, $p \leq 0.01$, $p \leq 0.001$ and $p \leq 0.0001$.

Immunocytochemistry (ICC). To assess the interaction of HCF with E-beam irradiated PMMA, we also studied the expression of specific cellular markers, including those indicative of adhesion, proliferation, and inflammation (Figure 7) using *ICC*. ALDH3A1 (keratocyte specific marker) expression was limited on both non-irradiated and irradiated (25 and 50 kGy) PMMA as previously shown.[29] Moreover, the expression of focal adhesion kinase (FAK), which is associated with cellular adhesion and spreading was similar for cells grown on non-irradiated and irradiated PMMA. The expression of integrin β1, which is associated with the cellular adhesion and interaction with the surrounding extra cellular matrix is also similar between groups. Thus, this expression pattern indicates that E-beam irradiation does not adversely impact cellular adhesion, or proliferation and spreading of HCF on PMMA. In addition, most HCF cultured on both non-irradiated and irradiated (25 and 50 kGy) PMMA expressed α–SMA, indicating a myofibroblast phenotype, which can be associated with fibrotic responses.[30]

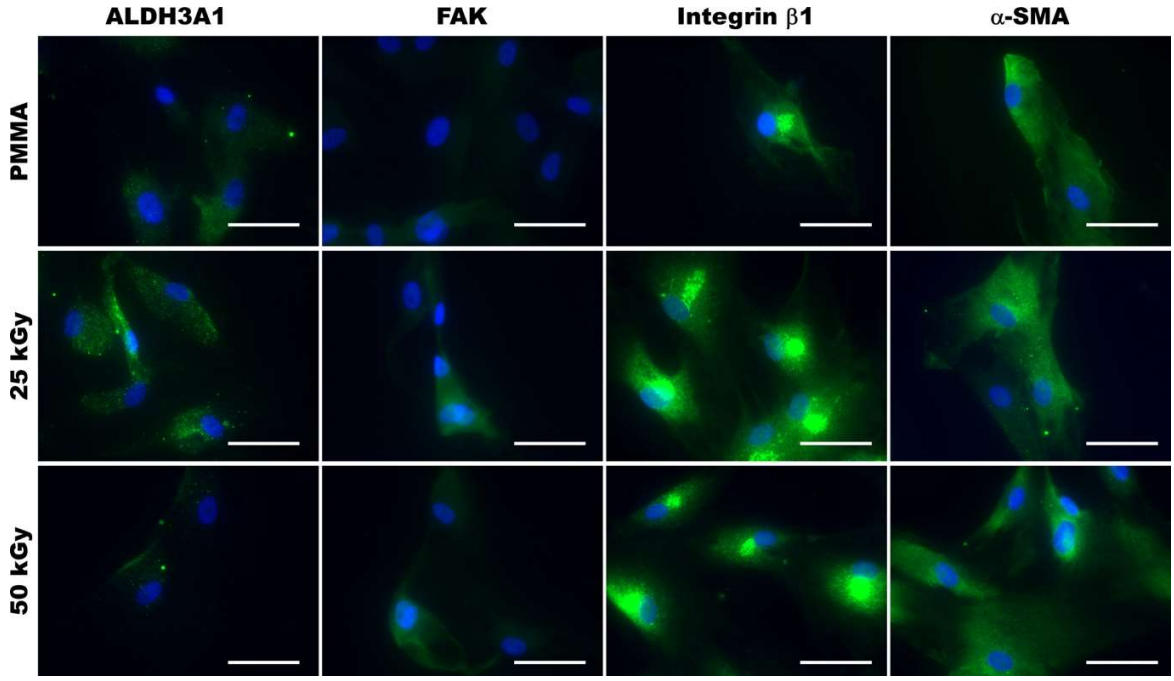

Figure 7. Representative immunofluorescence images of HCF cultured on non-irradiated or E-beam irradiated (25 and 50 kGy) PMMA for 7 days, and immunostained for ALDH3A1, focal adhesion kinase (FAK), integrin β1, and smooth muscle actin (α-SMA). Minimal variations were observed between cells grown on non-irradiated and irradiated PMMA. All cell nuclei were counterstained using DAPI (blue). Scale bar is 50 μm.

Complement Activation. Implanted materials are exposed to recognition molecules of the innate immune system including plasma cascades, of which the complement system is a central component, playing a key role in homeostasis, regeneration, and inflammation.[31] To assess complement activation, two activation fragments of the complement system were studied, C3bc and TCC (Figure 8). C3bc levels were similar between non-irradiated, and irradiated (25 and 50 kGy) PMMA, and to the background activation after 30 min incubation (T30), but higher in comparison to background activation of plasma immediately after blood draw (T0) ($p \leq 0.05$), as illustrated in Figure 8a. Soluble TCC levels are also similar between non-irradiated, irradiated (25 and 50 kGy) PMMA, and T30, and significantly higher than at T0 ($p \leq 0.0001$). These data suggest that complement activation can be attributed to the PMMA material and not to E-beam irradiation.

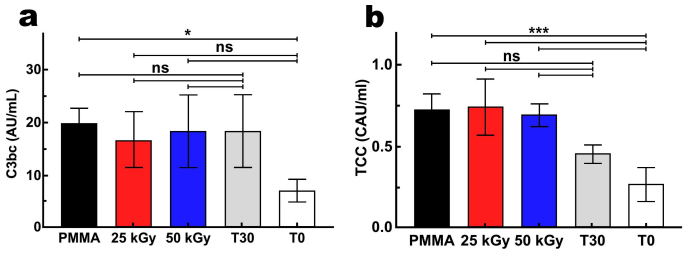

Figure 8. Complement activation of C3bc (**a**) and soluble terminal complement complex (TCC) (**b**) with or without E-beam irradiation compared to the background activation after 30 minutes (T30), and without incubation with PMMA (T0). The level of C3bc was statistically different only for T0; the latter represents the status of complement activation immediately after drawing blood from the donor. ns ($p > 0.05$), *$p \leq 0.05$, **$p \leq 0.01$, ***$p \leq 0.001$, and ****$p \leq 0.0001$.

In summary, we have shown that 25 kGy E-beam irradiation has a minimal impact on the chemical, mechanical, and optical properties of PMMA and has no apparent adverse effect on its biocompatibility with human corneal cells. These findings suggest that E-beam irradiation at 25 kGy may be a feasible sterilization alternative for PMMA used in medical implants. Future studies are required to determine the effect of E-beam sterilization *in vivo*.

Supporting Information

Supporting Information is available from the Elsevier Online Library or from the author.

Acknowledgements

This work was supported by a Barbara L. Crow Investigator-Concept Grant from Lions VisionGift, Portland, Oregon, and Boston Keratoprosthesis. R.S. was supported in part by EBAA/ Richard Lindstrom Research Grant (530720). This work was performed in part at the Center for Nanoscale Systems (CNS), Harvard University, a member of the National Nanotechnology Coordinated Infrastructure Network (NNCI), which is supported by the National Science Foundation under NSF award no. 1541959.

References:

[1] M. Haji-Saeid, M. H. O. Sampa, A. G. Chmielewski, *Radiation Physics and Chemistry* **2007**, *76*, 1535.

[2] L. Woo, C. L. Sandford, *Radiation Physics and Chemistry* **2002**, *63*, 845.

[3] a) J. G. Drobny, in *Ionizing Radiation and Polymers*, DOI: https://doi.org/10.1016/B978-1-4557-7881-2.00002-X (Ed: J. G. Drobny), William Andrew Publishing **2013**, p. 11; b) A. Chapiro, *Nuclear Instruments and Methods in Physics Research Section B: Beam Interactions with Materials and Atoms* **1988**, *32*, 111.

[4] R. G. Hill, in *Biomaterials, artificial organs and tissue engineering* (Eds: L. L. Hench, J. R. Jones), Woodhead Publishing **2005**, p. 97.

[5] a) B. F. Khan, M. Harissi-Dagher, D. M. Khan, C. H. Dohlman, *Int Ophthalmol Clin* **2007**, *47*, 61; b) S. Pujari, S. S. Siddique, C. H. Dohlman, J. Chodosh, *Cornea* **2011**, *30*, 1298.

[6] D. A. Atchison, *J Cataract Refract Surg* **1990**, *16*, 178.

[7] a) G. Lewis, *Journal of biomedical materials research. Part B, Applied biomaterials* **2017**, *105*, 1260; b) A. Gulec, M. A. Acar, B. K. Aydin, T. Demir, M. Ozkaya, *Proc Inst Mech Eng H* **2018**, *232*, 1025; c) D. Bourell, B. Stucker, D. Espalin, K. Arcaute, D. Rodriguez, F. Medina, M. Posner, R. Wicker, *Rapid Prototyping Journal* **2010**; d) M. Winking, J. P. Stahl, M. Oertel, R. Schnettler, D. K. Boker, *Ger Med Sci* **2003**, *1*, Doc08.

[8] U. S. F. a. D. Administration, Filling in wrinkles safely, https://www.fda.gov/consumers/consumer-updates/filling-wrinkles-safely, accessed.

[9] M. Silindir Gunay, Y. Ozer, *FABAD J Pharm Sci* **2009**, *34*, 43.

[10] a) G. Lewis, S. Mladsi, *Biomaterials* **1998**, *19*, 117; b) M. Gonzalez-Andrades, R. Sharifi, M. M. Islam, T. Divoux, M. Haist, E. I. Paschalis, L. Gelfand, S. Mamodaly, L. Di Cecilia, A. Cruzat, F. J. Ulm, J. Chodosh, F. Delori, C. H. Dohlman, *Ocul Surf* **2018**, *16*, 322.

[11] A. S. Traish, J. Chodosh, *Semin Ophthalmol* **2010**, *25*, 239.

[12] a) T. Munker, S. van de Vijfeijken, C. S. Mulder, V. Vespasiano, A. G. Becking, C. J. Kleverlaan, G. CranioSafe, G. CranioSafe, A. G. Becking, L. Dubois, L. H. E. Karssemakers, D. M. J. Milstein, S. van de Vijfeijken, P. Depauw, F. W. A. Hoefnagels, W. P. Vandertop, C. J. Kleverlaan, T. Munker, T. J. J. Maal, E. Nout, M. Riool, S. A. J. Zaat, *J Mech Behav Biomed Mater* **2018**, *81*, 168; b) R. M. Brinston, B. K. Wilson, *Med Device Technol* **1993**, *4*, 18; c) D. W. Meltzer, *J Am Intraocul Implant Soc* **1981**, *7*, 126.

[13] S. Urano, I. Wakamoto, T. Yamakawa, *Mitsubishi Heavy Industries Technical Review* **2003**, *40*, 1.

[14] D. W. Plester, *Effects of radiation sterilization on plastics*, Duke Univ Press, United States **1973**.

[15] L. K. Massey, in *The effect of sterilization methods on plastics and elastomers (second edition)* (Ed: L. K. Massey), William Andrew Publishing, Norwich, NY **2005**, p. 39.

[16] ASTM, in *ASTM D790-17*, West Conshohocken, PA 2017.

[17] a) J. M. Hackett, C. Ferguson, E. Dare, C. R. McLaughlin, M. Griffith, *Toxicology in Vitro* **2010**, *24*, 567; b) K. H. Chen, D. Azar, N. C. Joyce, *Cornea* **2001**, *20*, 731.

[18] a) S. Busschots, S. O'Toole, J. J. O'Leary, B. Stordal, *MethodsX* **2015**, *2*, 8; b) P. W. Madden, J. N. Lai, K. A. George, T. Giovenco, D. G. Harkin, T. V. Chirila, *Biomaterials* **2011**, *32*, 4076; c) S. I. Ivanova, S. Chakarov, A. Momchilova, R. Pankov, *Materials science & engineering. C, Materials for biological applications* **2017**, *78*, 230; d) R. Sharifi, S. Mahmoudzadeh, M. M. Islam, D. Koza, C. H. Dohlman, J. Chodosh, M. Gonzalez-Andrades, *Advanced Materials Interfaces* **2020**, *7*, 1900767.

[19] M. M. Islam, R. Sharifi, S. Mamodaly, R. Islam, D. Nahra, D. B. Abusamra, P. C. Hui, Y. Adibnia, M. Goulamaly, E. I. Paschalis, A. Cruzat, J. Kong, P. H. Nilsson, P. Argueso, T. E. Mollnes, J. Chodosh, C. H. Dohlman, M. Gonzalez-Andrades, *Acta biomaterialia* **2019**, *96*, 330.

[20] G. Bergseth, J. K. Ludviksen, M. Kirschfink, P. C. Giclas, B. Nilsson, T. E. Mollnes, *Mol Immunol* **2013**, *56*, 232.

[21] T. E. Mollnes, T. Lea, S. S. Froland, M. Harboe, *Scand J Immunol* **1985**, *22*, 197.

[22] P. Tiwari, A. K. Srivastava, B. Q. Khattak, S. Verma, A. Upadhyay, A. K. Sinha, T. Ganguli, G. S. Lodha, S. K. Deb, *AIP Conference Proceedings* **2012**, *1447*, 587.

[23] a) K. El-Salmawi, M. M. Abu Zeid, A. M. El-Naggar, M. Mamdouh, *Journal of Applied Polymer Science* **1999**, *72*, 509; b) R. L. Clough, K. Gillen, *Radiation-oxidation of polymers*, **1989**; c) M. Żenkiewicz, M. Rauchfleisz, J. Czupryńska, J. Polański, T. Karasiewicz, W. Engelgard, *Applied Surface Science* **2007**, *253*, 8992.

[24] N. W. Elshereksi, S. H. Mohamed, A. Arifin, Z. A. M. Ishak, **2014**, *25*.

[25] a) S. Barton, P. J. S. Foot, P. Tate, M. Kishi, B. Ghatora, *Polymers and Polymer Composites* **2013**, *21*, 1; b) T. Kohnen, *J Cataract Refract Surg* **1996**, *22 Suppl 2*, 1255.
[26] a) L. H. Sperlin, in *Introduction to Physical Polymer Science*, p. 349; b) S. Derbil, M. W. Khemici, N. Doulache, A. Gourari, N. Haine, *International Journal of Polymer Analysis and Characterization* **2017**, *22*, 622.
[27] N. Rashi, K. Anil, Y. K. Vijay, presented at 2007 IEEE Particle Accelerator Conference (PAC), 25-29 June 2007, **2007**.
[28] a) S. Mouaci, M. Saidi, N. Saidi-Amroun, in *Micro & Nano Letters*, Vol. 12, Institution of Engineering and Technology, 2017, 478; b) R. Dorati, M. Patrini, P. Perugini, F. Pavanetto, A. Stella, T. Modena, I. Genta, B. Conti, *Journal of Microencapsulation* **2006**, *23*, 123.
[29] R. Sharifi, S. Mahmoudzadeh, M. M. Islam, D. Koza, C. H. Dohlman, J. Chodosh, M. Gonzalez-Andrades, *Advanced Materials Interfaces n/a*, 1900767.
[30] M. Gonzalez-Andrades, J. de la Cruz Cardona, A. M. Ionescu, A. Campos, M. Del Mar Perez, M. Alaminos, *Invest Ophthalmol Vis Sci* **2011**, *52*, 215.
[31] a) K. N. Ekdahl, J. D. Lambris, H. Elwing, D. Ricklin, P. H. Nilsson, Y. Teramura, I. A. Nicholls, B. Nilsson, *Adv Drug Deliv Rev* **2011**, *63*, 1042; b) P. Schoengraf, J. D. Lambris, S. Recknagel, L. Kreja, A. Liedert, R. E. Brenner, M. Huber-Lang, A. Ignatius, *Immunobiology* **2013**, *218*, 1.